Structure
Article

A Left-Handed RNA Double Helix Bound by the Zα Domain of the RNA-Editing Enzyme ADAR1

Diana Placido,[1,2] Bernard A. Brown, II,[1,3] Ky Lowenhaupt,[1] Alexander Rich,[1] and Alekos Athanasiadis[1,*]
[1] Department of Biology, Massachusetts Institute of Technology, 77 Massachusetts Avenue, Cambridge, MA 02139, USA
[2] Present address: Instituto de Technologia Quimica e Biologica, Universidade Nova de Lisboa, 2781-901 Qeiras, Portugal.
[3] Present address: Wake Forest University, Department of Chemistry, Box 7486, 16A Salem Hall, Winston-Salem, North Carolina 27109-7486, USA.
*Correspondence: alekos@mit.edu
DOI 10.1016/j.str.2007.03.001

SUMMARY

The A form RNA double helix can be transformed to a left-handed helix, called Z-RNA. Currently, little is known about the detailed structural features of Z-RNA or its involvement in cellular processes. The discovery that certain interferon-response proteins have domains that can stabilize Z-RNA as well as Z-DNA opens the way for the study of Z-RNA. Here, we present the 2.25 Å crystal structure of the Zα domain of the RNA-editing enzyme ADAR1 (double-stranded RNA adenosine deaminase) complexed to a dUr(CG)$_3$ duplex RNA. The Z-RNA helix is associated with a unique solvent pattern that distinguishes it from the otherwise similar conformation of Z-DNA. Based on the structure, we propose a model suggesting how differences in solvation lead to two types of Z-RNA structures. The interaction of Zα with Z-RNA demonstrates how the interferon-induced isoform of ADAR1 could be targeted toward selected dsRNAs containing purine-pyrimidine repeats, possibly of viral origin.

INTRODUCTION

The main difference between DNA and RNA is the presence of the ribose 2′-OH groups; however, this difference makes the two macromolecules very different with regard to their biochemical behavior as well as the structures they adopt as double helices. B-DNA and A-RNA, fundamentally different in structure, are recognized by distinct and generally nonoverlapping sets of protein domains. Nevertheless, both nucleic acid double helices can undergo a transition to left-handed double-helical structures, referred to as Z-DNA (Wang et al., 1979) and Z-RNA (Hall et al., 1984). Z-DNA is a well-characterized DNA structure stabilized in vivo by negative supercoiling occurring during transcription (Liu and Wang, 1987; Wittig et al., 1991) and in vitro by high-salt conditions (Pohl and Jovin, 1972). However, the A-to-Z transition of dsRNA in vitro requires higher salt concentrations and higher temperature than the equivalent B-to-Z transition of dsDNA, indicating that Z-DNA is energetically more favorable than Z-RNA (Hall et al., 1984). Despite that, staining with antibodies against Z-RNA suggests its extensive presence both in the cytoplasm and the nucleolus (Zarling et al., 1990). Structural information on Z-RNA comes from the crystallographic analysis of chemically modified or chimeric RNAs (Nakamura et al., 1985; Teng et al., 1989) or solution studies in the presence of 6 M concentrations of $NaClO_4$ (Davis et al., 1990; Popenda et al., 2004). The latter showed that left-handed RNA helices in this environment are drastically different from Z-DNA, contrary to earlier interpretations pointing to similar Z-DNA and Z-RNA conformations. Extensive analysis involving CD, Raman, and NMR spectroscopy indicate that more than one species of Z-RNA may exist (Trulson et al., 1987). However, what is needed is an explanation of the observed discrepancies and a characterization of Z-RNA in a likely in vivo environment.

An indication of a distinct biological role for Z-DNA came with the discovery of a conserved domain (Zα), part of the vertebrate RNA-editing enzyme ADAR1, which binds specifically and with high affinity to Z-DNA both in vitro and in vivo (Herbert et al., 1997; Kim et al., 2004; Schwartz et al., 1999). Further, it was discovered that $Z\alpha^{ADAR1}$ would also bind to Z-RNA, as seen in circular dichroism studies of the dsRNA A-to-Z transition (Brown et al., 2000). Since the discovery of $Z\alpha^{ADAR1}$, Z-DNA-binding domains (Z domains) have been found in a number of proteins whose common feature is that they either participate in the interferon-response pathway (DLM-1, PKZ) (Rothenburg et al., 2005; Schwartz et al., 2001) or are viral inhibitors of this pathway (E3L) (Kahmann et al., 2004). The activation of the interferon-response pathway is initiated by the detection of viral dsRNA. PKR in higher organisms possesses two dsRNA-binding domains (dsRBDs) that mediate its activation (Robertson and Mathews, 1996), while in certain fish species whose genomes have been analyzed the only known analog is PKZ, a protein that contains two Z domains instead of dsRBDs (Rothenburg et al., 2005). Thus, it is reasonable to ask whether some Z domains are targeted to Z-RNA rather than Z-DNA. More importantly, ADAR1, but not ADAR2 (which does not contain a Z domain), edits dsRNA substrates in vitro at significantly higher levels when they contain Z-forming purine-pyrimidine repeats (Koeris et al., 2005). Functionally, the

interferon-induced form of ADAR1 has been associated with RNA editing of a wide array of viral genomes, including the measles virus and hepatitis C and D viruses (Cattaneo, 1994; Horikami and Moyer, 1995; Polson et al., 1996; Taylor et al., 2005).

Circular dichroism studies have indicated that the ADAR1 Zα domain promotes the A-to-Z transition of dsRNA in a near physiological environment (Brown et al., 2000). In the present work, we ask whether $Z\alpha^{ADAR1}$ binds to Z-RNA in a manner similar to its binding to Z-DNA, and whether specific interactions with the RNA 2′-OH groups are formed that might suggest a preference for Z-RNA. At the same time, $Z\alpha^{ADAR1}$ provides an excellent tool for the structural analysis of Z-RNA at near physiological ionic strength conditions, and it could provide answers to long-standing questions regarding the structure of Z-RNA.

Here, we present the 2.25 Å structure of a complex of $Z\alpha^{ADAR1}$ with $dUr(CG)_3$ dsRNA. We show that Zα binds left-handed Z-RNA at low-salt and low-temperature conditions, and we compare its binding to Z-DNA. The structure shows defining features of the left-handed RNA conformation and provides an explanation for the spectroscopic studies of Z-RNA, indicating the existence of more than one Z-RNA species. The structure of the complex shows that Zα is a Z-RNA-binding module with relevance to a number of proteins involved in interferon response.

RESULTS

The Zα/Z-RNA Complex

We determined the structure of the Zα domain from human ADAR1 complexed with a $dUr(CG)_3$ duplex oligonucleotide at 2.25 Å resolution (for statistics, see Table 1). In the asymmetric unit, two similar (rms distance of 0.54 Å) Zα monomers are bound to the Z-RNA duplex, and each Zα monomer interacts with a single RNA strand (Figure 1). Since there are no contacts between Zα monomers, dimerization does not appear to be a prerequisite for binding, similar to what has been seen for the interaction of Zα with Z-DNA (Schwartz et al., 1999). The interaction between two crystallographically related monomers (blue and red on the upper part of Figure 1) is characterized by a buried surface of 253 $Å^2$ and very few intermolecular interactions, suggesting that it rather represents a typical crystal contact and not a biologically relevant dimeric molecular interaction. The overall domain fold and the mode of the interaction with the nucleic acid backbone are well conserved between the Zα/Z-DNA and Zα/Z-RNA complexes. The protein maintains its helix-turn-helix fold with a β sheet, and nucleic acid interactions are made by residues from the recognition helix and the β sheet. Five successive phosphates on the Z-RNA backbone are involved in protein-RNA hydrogen bonding. However, in contrast to the Zα/Z-DNA structures, which show a pseudo continuous helix along the crystal, the Z-RNA duplexes in our structure are arranged with a 90° angle between each segment, and, interestingly, the overhanging dU base of the duplex stacks onto the helix of a neighboring symmetric dsRNA (Figure 1). Modeling of a ribose 2′ hydroxyl group on the dU overhang shows that its presence would sterically inhibit the observed base stacking, offering an explanation for the requirement of the dU overhang for crystallization.

Direct hydrogen bonding interactions with the RNA backbone are formed by Tyr177, Asn173, Lys169, and Lys170 from the recognition helix and Thr191 from the β sheet turn (Figure 2) and are directed to phosphate oxygens as well as the O4 of a ribose ring. The residues Asn173, Trp195, and Lys187 contribute to interactions with solvent-mediated hydrogen bonds. Both Zα monomers each interact with one RNA strand in a very similar manner. The most notable difference between the Zα/Z-DNA and Zα/Z-RNA complexes is the lack of interaction of Arg174, which in the Z-DNA structure provides a hydrogen bond to the phosphate oxygen of C5, while in the RNA structure points away from the RNA and forms a crystal-packing interaction. However, as Arg174 is not particularly

Table 1. Data Collection and Refinement Statistics of the Zα/Z-RNA Complex

Data Collection and Processing	
Resolution	25–2.25 Å
Space group	$C222_1$; a = 73.60 Å, b = 92.77 Å, c = 50.23 Å, α = β = γ = 90°
R_{sym} (%)	7.5 (19.7)[a]
Completeness (%)	90.7 (92.5)[a]
Multiplicity	5.1 (5.1)[a]
Observed reflections	38,204 (3,383)[a]
Unique reflections	7,511 (660)[a]
Wavelength	0.97 Å
Refinement	
R factor for all reflections (%)	19.9
R factor working set (%)	19.4 (21.6)[a]
R_{free} (%) for 9.7% of reflections	24.7 (36.4)[a]
Reflections (working set)	6,769
Reflections (test set)	730
Nonhydrogen atoms	1,406
Average atomic B factor (protein)	23.7 $Å^2$
Average atomic B factor (RNA)	21.6 $Å^2$
Average atomic B factor (solvent)	26.9 $Å^2$
Solvent molecules	157 waters, 3 Na^+
Rms bond distances	0.007 Å
Rms bond angles	1.198°
Rms chiral center restraints	0.053 $Å^3$

[a] Statistics in parentheses are for the outer-resolution shell: 2.31–2.25 Å.

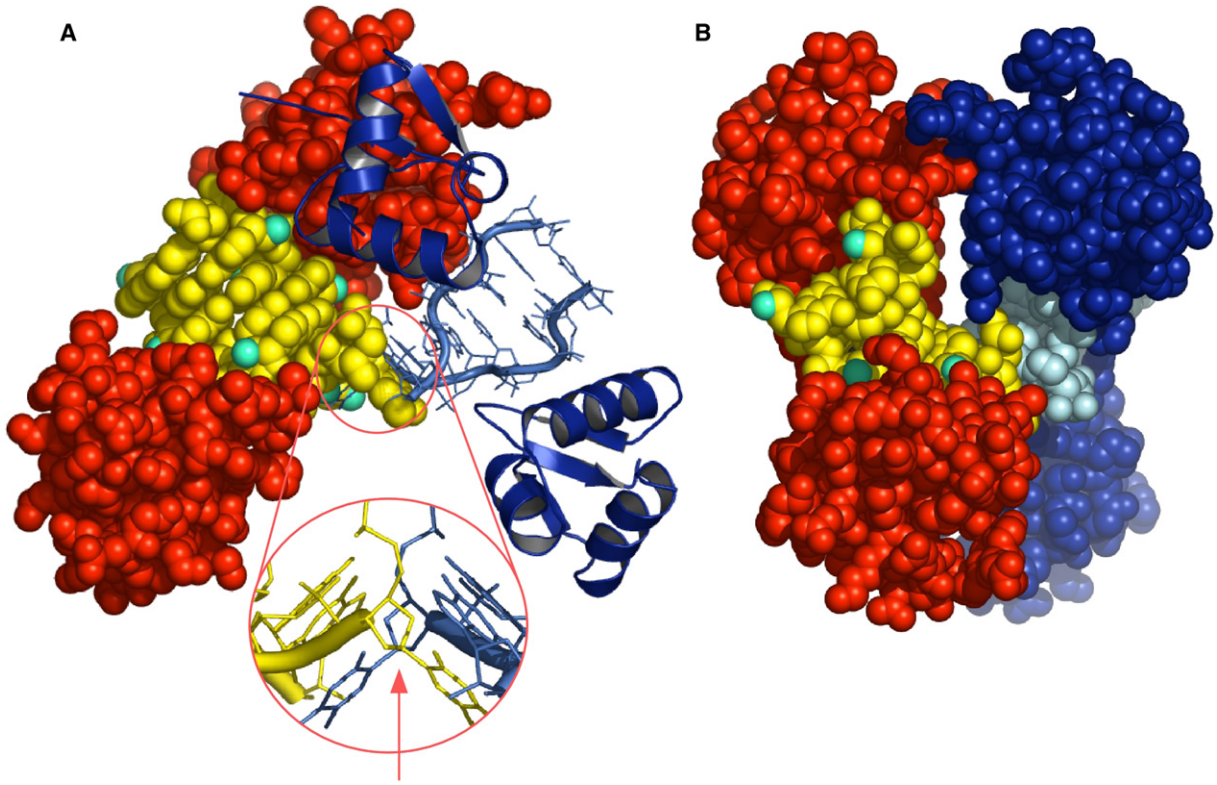

Figure 1. Overall Structure of the Zα/Z-RNA Complex

(A) The asymmetric unit has two noninteracting Zα monomers (red space-filling model) bound to a $dUr(CG)_3$ Z-RNA duplex. A second symmetry-related complex is displayed as structural motifs. The overhanging deoxy-uridine base of each duplex is stacked onto the neighboring Z-RNA molecule related by crystallographic symmetry, as seen in the magnification. The Zα domain is a typical winged-helix-turn-helix domain, and it contacts five Z-RNA phosphates with residues from its recognition helix and the β sheet turn. The presence of the RNA 2′-OH groups (cyan spheres) does not hinder the interactions previously seen between Zα and a Z-DNA helix; instead, the 2′-OH groups participate in the interface by forming water-mediated hydrogen bonds to the protein. The arrow indicates the two-fold symmetry axis that relates the two complexes.

(B) A rotated view around the y axis of the all space-filling model reveals that the interface between the symmetry-related monomers (blue and red) on the top is limited and likely represents a crystal contact.

conserved among Zα sequences, loss of this hydrogen bond in the cocrystal appears to not have a significant effect in binding RNA.

Despite very different crystal packing, overall the Zα/Z-RNA complex is very similar to the complex of Zα with Z-DNA. Our analysis thus concentrates on the features that are unique in RNA: namely, the ribose 2′-OH groups. Our initial expectation had been that specificity interactions for RNA might be achieved through direct contacts of the protein with the 2′ hydroxyl groups. However, the cytosine 2′-OH groups are deeply buried in the minor groove and not available for protein/Z-RNA contacts, leaving guanosine 2′-OH as the only candidate for interaction. The G2 2′-OH forms a water-mediated contact to Tyr177 (Figures 2A and 2B) in both monomers, and the G4 2′-OH forms a water-mediated hydrogen bond to the backbone O of Arg174. We observe no direct protein contacts with the exposed guanosine 2′-OH RNA groups. Thus, if Zα distinguishes Z-RNA from Z-DNA, it does so through the additional stability conferred by these water-mediated interactions.

We had previously observed that one of the water molecules mediating the interaction of one C3 phosphate oxygen with two absolutely conserved residues of the Z domain family (Trp195 and Asn173) is present in all Z domain structures, even in the absence of DNA and with low B factors (Athanasiadis et al., 2005). Based on these observations, we speculated on the importance of this solvent position for the stability of the domain and its interaction with nucleic acids. In the refinement of the Zα/Z-RNA structure, this possible water converged to a temperature factor (~4 $Å^2$) much lower than that of the protein and RNA atoms (12.6 $Å^2$) that surround it and to which it is hydrogen bonded (represented as Na^+ in Figure 2). This suggested that this position may in fact be occupied by a metal ion. Considering the crystallization conditions and the electron density of the observed peak, we concluded that this position is a Na^+ ion (see Experimental Procedures). The water molecules occupying the same position in all other Z domain structures display less striking but also low B factors (10–20 $Å^2$), and it is possible that they represent misinterpreted Na^+ ions. This is not

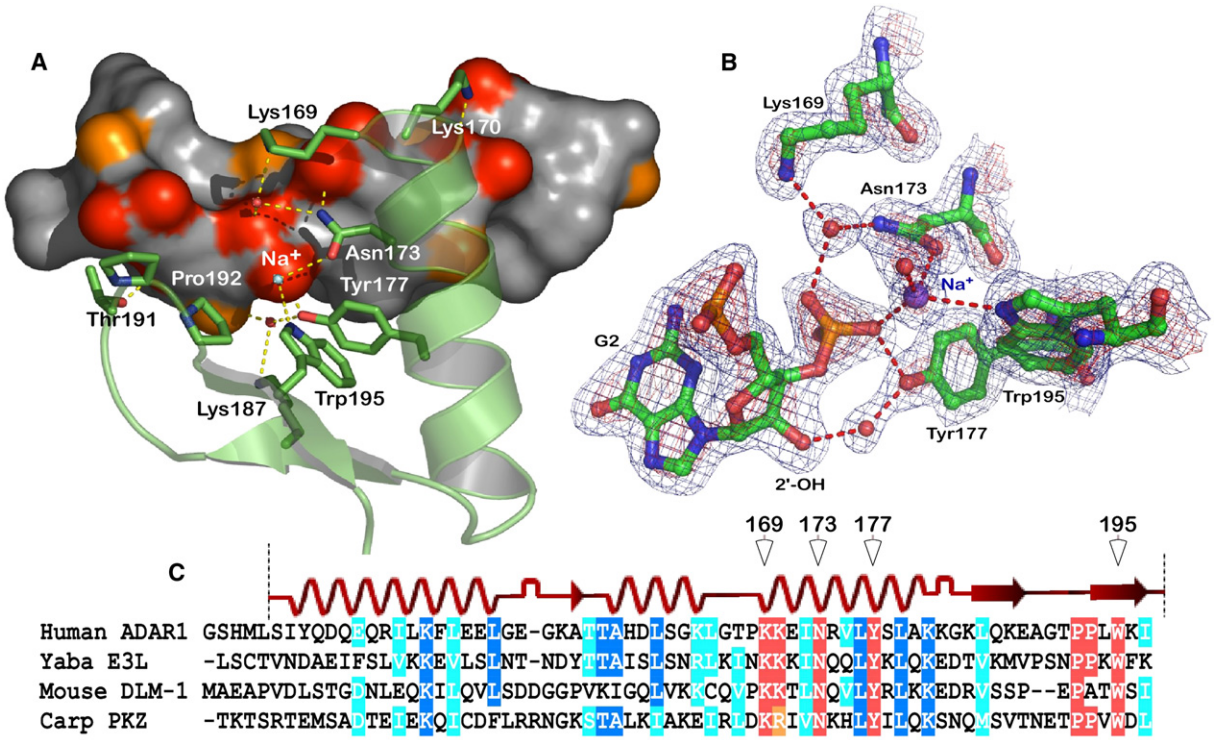

Figure 2. The Zα/Z-RNA Interface

(A) The water-accessible surface of a single RNA strand (gray) as well as the Zα residues that form contacts with the RNA backbone are illustrated. On the surface, ribose 2′ hydroxyl groups are shown in orange, and phosphate oxygen atoms are shown in red. All but one of the Zα direct contacts are with phosphate oxygen atoms; Thr191 is hydrogen bonded to ribose O4. Small spheres represent water molecules (red). A candidate sodium ion (gray) has a central position in the interaction. The second RNA strand, omitted for clarity, is not contacted by this Zα monomer; it has almost identical contacts with a second Zα monomer.

(B) Electron density map ($2F_o - F_c$) contoured at 1σ (blue) and 3σ (red) of guanine 2 and Zα residues that form Z-RNA-specific, solvent-mediated contacts. Red spheres represent water molecules, and red, dotted lines represent hydrogen bonds. A sodium ion is shown in purple.

(C) Sequence alignment of representative Zα domains whose three-dimensional structure in complex with Z-DNA is known (1QBJ for ADAR1, 1SFU for E3L, and 1J75 for DLM-1) and of the Zα domain of PKZ, the PKR homolog. Conserved residues that form critical contacts with the RNA are highlighted red, while other conserved residues (mainly hydrophobic core residues) are highlighted blue.

surprising as at nonatomic resolution the electron difference between O and Na^+ is too small to be unambiguously distinguished because the thermal displacement of the ion can usually mask its electron number difference. The ion displays a tetrahedral coordination and distances (2.5–3.1 Å) from its neighboring atoms, relatively short for water and long for other biologically relevant metal ions such as Zn^{2+} or Mg^{2+}. We also considered the possibility that, due to the acidic conditions of the crystallization, phosphate oxygens are to some extent protonated and this position is occupied by a chloride ion. Such a possibility however contradicts with the fact that most Zα RNA interactions are identical to those of Zα in complex with DNA occurring at higher pH. If an extensive protonation of the phosphate oxygens was present at our crystallization conditions, Lys169 and Lys170 would not contribute with favorable interactions, and it is highly unlikely that the Zα/RNA complex would form. Moreover, the ion resides closer to the phosphate oxygen (2.5 Å) than to the Trp NE1 atom (3.1 Å), suggesting that a sodium ion is most likely occupying this position. Such an interaction of a Trp NE1 with a metal ion at low pH values would suggest that the three invariant Zα residues (Tyr177, Asn173, and Trp195) interacting with the two closely approaching RNA phosphate groups form a highly polarized pocket. The central position of the ion in the binding pocket and its invariant interaction pose some intriguing questions regarding its role in the interaction of Zα with Z form nucleic acids.

The Z-RNA Conformation

To our knowledge, this is the first structure determined by X-ray crystallography that displays dsRNA in its left-handed conformation and is the first structure of Z-RNA at low-salt conditions. Thus, it provides an opportunity to define the differences between the Z-RNA conformation and its Z-DNA relative and to identify changes associated with the high-salt environment found in the NMR structure in 6 M $NaClO_4$ (Popenda et al., 2004).

The helical parameters for Z-RNA in our complex closely follow those that have been previously observed crystallographically for Z-DNA (Wang et al., 1979). In particular, the helical twist angles average −8.6° for CpG

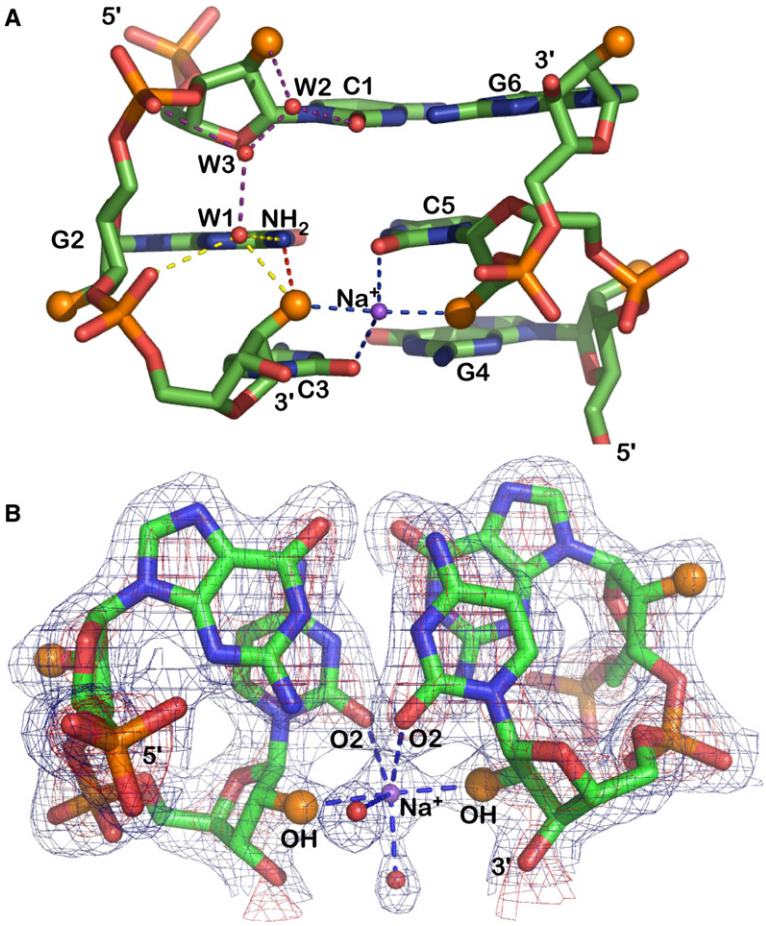

Figure 3. Hydration of the RNA Backbone

(A) The 2′ hydroxyl groups (larger orange spheres) participate in four distinct interactions: (i) with guanine NH_2 (red, vertical dash); (ii) as a sodium bridge to the opposite-strand 2′ hydroxyl (horizontal, blue dash); (iii) with a water (W1) linked to the 5′ phosphate group (yellow dash); and (iv) as shown for cytosine C1, with the 3′ phosphate group (purple dash), in an interaction linked through waters W2 and W3. The water pattern associated with only one strand is shown, but a similar water pattern is observed for all residues.

(B) Electron density ($2F_o - F_c$) of a GpC step and the Na^+ bridging 2′ ribose hydroxyl groups of opposing strands. The map is contoured at 1σ (blue) and 3σ (red) levels.

steps and −50.9° for GpC steps. This is associated with base stacking in CpG steps, which is interstrand with G residues stacking over the ribose moiety of cytidines (Figure 4E); however, it is entirely intrastrand for GpC steps (Figures 3B and 4B). This stacking is very different from that adopted by Z-RNA under high-salt conditions (Popenda et al., 2004), where intrastrand stacking is observed for CpG steps (for comparison of base stacking, see Figures 4E and 4F). The ribose moieties of Z-RNA adopt a C2′-endo puckering for cytidine residues and a C3′-endo puckering for guanosines, as has been seen for Z-DNA. The sole exception is the 3′-terminal guanosine of one strand, which shows C2′-endo conformation (see Table S1 in the Supplemental Data available with this article online). For both the Zα/Z-RNA and Zα/Z-DNA complexes we observe the same sugar pucker preferences, with the exception that in the Zα/Z-DNA complex, the 3′-terminal guanosine of both strands adopts a C2′-endo conformation. It is apparent that terminal nucleotides have more degrees of freedom and are under the influence of crystal-packing interactions. In contrast, in the high-salt NMR structure of Z-RNA, it is found that most G residues adopt a C4′-exo puckering, while cytidines adopt C2′-endo, C3′-exo, or C1′-exo puckering. Based on the NMR structure under high-salt conditions, it has been proposed that Z-RNA represents a novel left-handed helix significantly different from Z-DNA (Popenda et al., 2004). Our results are not consistent with such a notion, but rather point to significant conformational changes of the Z-RNA helix induced by high salt. As discussed in the next section, this change in conformation is related to a collapsed solvation structure. A detailed analysis of the torsion angles defining the sugar conformation (see Table S2) suggests that Z-RNA in our structure is closest to the typical Z_I species of Z conformations (Wang et al., 1981).

The Role of 2′-OH Groups

Ribose 2′ hydroxyl groups are a central feature in the chemical and structural properties of RNA; thus, we carefully examined their role in the Z-RNA structure. It has been postulated that the cytidine 2′-OH groups play an important role in the stability of Z-RNA, forming intrastrand hydrogen bonds with the NH_2 groups of the preceding guanosine residue (Teng et al., 1989). Such an interaction was observed in a high-salt NMR structure of $r(CG)_3$ (Popenda et al., 2004) and is also present in our structure (Figure 3A). This is an important stabilizing interaction as all distances we observe for this interaction fall in the range of 3–3.2 Å, favorable for hydrogen bond formation.

On the other hand, the direct interstrand contact between cytidine 2′-OH groups observed in the high-salt NMR structure of Z-RNA (Figure 4C) is not seen in the

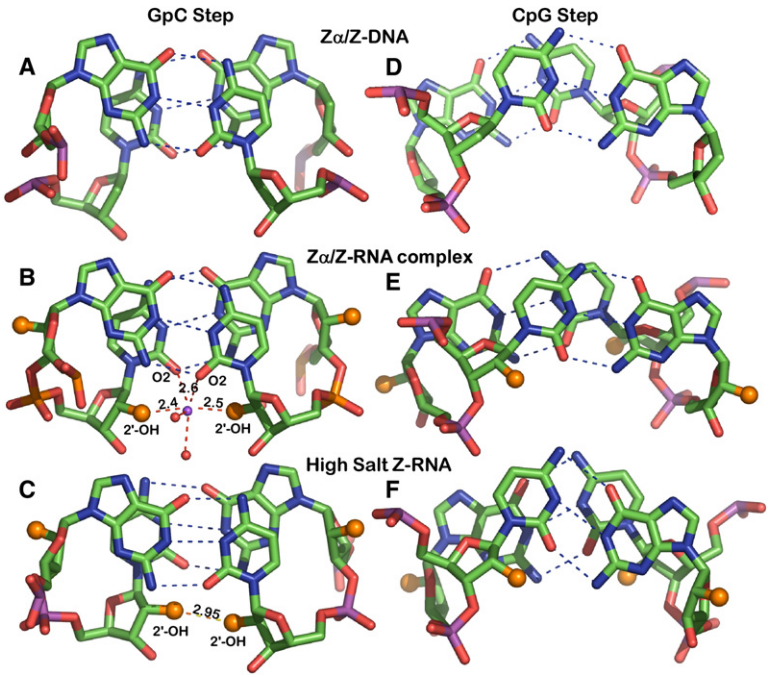

Figure 4. Base Stacking and Backbone Hydration of the Two Z-RNA Conformations and that of Z-DNA

(A–F) (A and D) Z-DNA, (B and E) Z-RNA cocrystal (this work), and (C and F) NMR structure of Z-RNA in 6 M $NaClO_4$. Dashes show Watson-Crick hydrogen bonding (blue) and 2′-OH hydrogen bonds (red/orange). The 2′-OH groups are displayed as larger orange spheres. The Z-DNA model is from the Zα/Z-DNA complex (Schwartz et al., 1999), and the high-salt Z-RNA structure is from the NMR study in 6 M $NaClO_4$ (Popenda et al., 2004). Distances are given in Angstroms. Note the overall similarity and the (D and E) interstrand base stacking of CpG steps in the Zα/Z-DNA and Zα/Z-RNA complexes, as opposed to (F) intrastrand stacking in high-salt RNA.

Zα/Z-RNA complex (Figures 3A, 3B, and 4B). The distance between the hydroxyl groups seen in the crystal is 4.7–4.8 Å, compared with the 2.9–3.1 Å distance seen in the high-salt Z-RNA, which results in a significant (~2 Å) difference in the minor groove dimensions. In the Zα/Z-RNA structure, the space between the opposite-strand 2′-OH groups is occupied by Na^+ ions (Figures 3A, 3B, and 4B), as the stereochemistry of the site suggests. The sodium ions form a four-way bridge that includes the cytosine base O2 atoms, and they occupy a position that coincides with the helical axis. Under high-ionic strength conditions, the 2′-OH groups from opposing strands move 2 Å closer, making a direct interaction, and Na^+ ions are expelled from the core of the RNA backbone. However, such a movement cannot be achieved without major alterations throughout the helix.

Two additional interactions of the ribose 2′-OH groups are with waters W1 and W2, which run along the RNA backbone and link the 2′ hydroxyls with the 5′ and 3′ phosphate groups, respectively, and eventually to each other through water W3 (Figure 3A). The cytosine 2′ hydroxyl groups form the foundation of a regular and apparently stable hydration pattern both along the Z-RNA helix and across its minor groove. This is likely to have a significant positive effect on the stability of Z-RNA. Systematically bound waters are also seen in Z-DNA structures (Gessner et al., 1989); however, in the case of Z-RNA, the 2′-OH groups lead to higher organization by interconnecting otherwise isolated interactions. In the Zα/Z-DNA structure, waters occupying the equivalent position of water W1 are consistently present and are bound by the guanosine NH_2 and the neighboring phosphate oxygen, W2 waters are consistently absent, and finally W3 waters can occasionally be found. None of these backbone waters or the sodium ions are being contacted by Zα; thus, the characteristic solvation of the Z-RNA backbone does not present a discriminating surface for Zα.

The guanosine 2′-OH groups on the other hand are exposed on the surface of Z-RNA and are not expected to significantly affect Z-RNA stability (Figure 3). However, they could be a major feature that would distinguish Z-RNA from Z-DNA for any interacting molecule.

DISCUSSION

Z-RNA Recognition by Zα

In the $dUr(CG)_3$ Z-RNA structure, the cytidine hydroxyl groups are hidden in a very narrow minor groove, and no contacts with protein groups are observed. On the other hand, guanosine 2′ hydroxyls are exposed on the outer surface of the helix. Among the three guanosine hydroxyl groups only that of G2 is contacted by a Zα side chain through a water bridge to Tyr177 (Figure 2). It is difficult to evaluate the importance of such a water-mediated interaction: Zα forms only six direct hydrogen-bonding interactions to Z-DNA; thus, one additional hydrogen bond could have a significant effect on stability, but the positional flexibility of water molecules probably limits the recognition capacity of such an interaction. Tyrosine 177 plays a central role in the recognition of the Z conformation, as its ring forms an edge-to-face π bond with the Z-DNA/Z-RNA-specific guanosine in the syn conformation as well as a direct hydrogen bond with the phosphate oxygen. Thus, it is not surprising that Tyr177 mutants abolish Z-DNA binding (Schade et al., 1999). In the Zα/Z-RNA complex, it additionally forms a water-mediated bond to the ribose 2′ hydroxyl. Overall, our conclusion is that RNA and DNA are similarly suited as ligands of the ADAR1 Zα domain, and that the small differences observed in the binding constants (Brown et al., 2000)

probably reflect differences in the B-to-Z and A-to-Z equilibria rather than a binding preference of Zα for the left-handed nucleic acid helix. Clearly, this makes the Zα domain one of the few protein domains able to bind dsDNA and dsRNA of the same sequence, both in the left-handed conformation.

The ADAR1 Zα domain is present in the interferon-induced and cytoplasmic/shuttling isoform of the enzyme, but it is absent from its constitutive and nuclear protein (George and Samuel, 1999). It is believed that the interferon version of ADAR1 (iADAR1) serves an antiviral role. Indeed, several RNA viruses show A-to-I genomic hypermutation in persistent infections (Cattaneo, 1994; Horikami and Moyer, 1995). Hepatitis D virus employs editing by ADAR1 as a switching mechanism between the early and late stages of its life cycle (Polson et al., 1996). Moreover, replicons of Hepatitis C are suppressed by this RNA-editing enzyme (Taylor et al., 2005). ADAR1 has three dsRBDs that can target this enzyme to double-stranded RNA regions of viruses, i.e. genomic RNA, or regular transcripts with double-stranded regions. At this point, it is not clear what the Z-RNA-binding domain (Zα) may confer, in addition, for the recognition of viral RNA. It is possible that induction of Z-RNA is the result of negative supercoiling introduced by viral replication, as has been shown to be the case for cellular transcription (Wittig et al., 1991). In such an event, Zα could serve to direct ADAR1 specifically to negatively supercoiled viral components, reducing in this way the effect the enzyme may have on cellular mRNA transcripts or noncoding RNAs bearing double-stranded regions. Indeed, there is significant evidence suggesting that ADARs can interfere with crucial dsRNA pathways such as RNA silencing and micro-RNA-mediated regulation (Scadden, 2005; Tonkin and Bass, 2003). During upregulation by interferon, the coexistence of full-length ADAR1 in the cytoplasm along with the RISC complex could potentially have implications for cytoplasmic RNA processing.

Evidence for the ability of the Zα domain to target ADAR1 activity on RNAs with Z-forming sequences was provided in a recent in vitro work in which the editing levels of double-stranded RNAs bearing CG repeats were significantly elevated over RNAs without such Z-forming sequences when exposed to full-length ADAR1. No such increase in editing was observed when exposed to ADAR2, which does not contain Z domains (Koeris et al., 2005). Similarly, full-length ADAR1 was shown to bind siRNAs with much higher affinity than the short ADAR1 form lacking Zα, although the mechanism underlying this increase in affinity is unclear so far (Yang et al., 2005).

Zα domains are also found in the interferon response-related protein PKZ. PKZ is a close relative of PKR that can be found in several fish species. It differs from PKR in that it has Z domains instead of the dsRBDs normally found; however, it does maintain an intact kinase domain. Normally, PKR detects the presence of viral dsRNA through its dsRBDs, which leads to the activation of the kinase domain by auto-phosphorylation. PKR then phosphorylates the eukaryotic initiation factor 2a (eIF2a), resulting in a shutdown of cellular translation (Robertson and Mathews, 1996). It is reasonable to assume that the Zα domains play similar roles in PKZ targeting of replicating viral RNAs, as it also phosphorylates eIF2a in the same position. For several dsRBDs, including those of ADAR2, recognition of specific structural features of complex RNA structures plays an important role in their selectivity of substrates (Stefl et al., 2006; Liu et al., 2000). Thus, it is becoming increasingly evident that the long-held assumption that dsRBD domains are general dsRBDs with no binding specificity is at least inaccurate. The presence of Z domains in PKZ, instead of dsRBDs in PKR, suggests that they are both activated by dsRNA, one by right handed and the other by left handed. They are both signals showing that the cell is infected by a virus. PKR recognizes viral transcripts bearing regions of dsRNA, while PKZ may recognize the process of making viral RNA by detecting negative torsional-strained RNA formed during replication. Thus, the roles postulated for the $Z\alpha^{ADAR1}$ and the $Z\alpha^{PKZ}$ domains may be fundamentally very similar. The structure of Zα complexed to Z-RNA provides evidence for the stability of this interaction, describes how a Z domain binds Z-RNA, and provides the first, to our knowledge, view of left-handed RNA in biologically relevant conditions.

Solvation Stabilizes Z-RNA, and Differences in Solvation Lead to Two Distinct Forms of Z-RNA

The crystal structure of the first protein-Z-RNA complex presented here shows that Z-RNA is conformationally very similar to Z-DNA, and its structure does not appear to be disturbed by protein binding (Figures 4A, 4B, 4D, and 4E). However, despite their conformational similarities, the two left-handed helices differ significantly in their solvation pattern, largely due to the presence of the cytosine 2′-OH groups.

Comparing Z-RNA stabilized by Zα binding to the high-salt NMR structure reveals drastic conformational changes (Figure 4). The most striking change is the closing of the minor groove by 2 Å in the high-salt structure (Figures 4B and 4C). This movement allows cytosine 2′-OH groups on opposing strands to form a hydrogen bond with each other. In the Zα cocrystal structure, a sodium ion is forming a four-way interstrand bridge between those 2′-OH groups. It appears paradoxical that a concentration of 6 M $NaClO_4$ leads to the removal of sodium ions from the RNA backbone. An explanation for this behavior may rest on the geometry of the low-salt binding site: cytosine 2′-OH groups are located at opposing positions and at a distance of 2.3–2.5 Å from the metal ion. However, at high ionic strengths, and due to decreased phosphate repulsion between strands, perturbation of the RNA backbone would make it unfavorable to retain the Na^+ ions. The conformation of nucleic acids is dominated by the repulsion of negatively charged phosphate groups. For example, the conversion of poly(dC-dG) from B-DNA to Z-DNA occurs in 4 M NaCl (Pohl and Jovin, 1972). The high-salt concentration shields the repulsion between charged phosphate groups, and the P-P distances in

Z-DNA are shorter than in B-DNA (Wang et al., 1979). Here, we compare the conformation of Z-RNA in 0.1 M Na^+ versus 6 M Na^+. The higher Na^+ concentration shields phosphate-phosphate repulsions, leading to lower P-P distances for CpG steps and even lower distances for the interstrand phosphate contact in 6 M Na^+ (on average: 6.1 Å for CpG, 6.3 Å for GpC, and 6.7 Å for the interstrand contact) compared to 0.1 M Na^+ (6.5 Å for CpG, 6.0 Å for GpC, and 7.6 Å for the interstrand contact). The shorter P-P distances in 6 M Na^+ changes the conformation of the nucleotides, driving together the cytosines on opposing chains and eliminating the Na^+-binding site formed in the 0.1 M Na^+ structure.

Adjustment to the new backbone conformation leads to the differences of base stacking and ribose puckering (Figures 4E and 4F). In the CpG steps, the low-salt Z-RNA structure shows cytidines stacked over opposite-strand cytidines, while the high-salt structure shows only interstrand stacking. The differences in ribose conformation are difficult to observe in Figure 4 but become clear by comparing their conformational parameters (Table S1).

Biochemical and spectroscopic analysis of Z-RNA has led to the proposal of the existence of two forms of Z-RNA, which have been termed Z_D and Z_R (Trulson et al., 1987), but their structural differences are not defined. Z_D is ascribed a Z-DNA-like conformation, while Z_R is presumed to be a novel, but still left-handed, helix. Consistent with this assessment, the Z-RNA bound to Zα in the cocrystal structure resembles Z-DNA and possibly represents the Z_D structure, while the high-salt NMR structure is likely to be responsible for the Z_R spectroscopic behavior. The two Z-RNA forms have been observed spectroscopically as a result of using different salts to induce Z-RNA formation: $MgCl_2$ for Z_D and NaBr or $NaClO_4$ for Z_R (Trulson et al., 1987). If the driving force behind the two conformations is ionic strength, then it is likely that titration with a single salt would result initially in an A-to-Z_D transition, followed later by a Z_D-to-Z_R transition. Unfortunately, in most studies only the final state has been fully analyzed; however, in at least one case, Z_D was found to be present along with A-RNA at low ionic strength and to be replaced by Z_R at higher ionic strengths (Hardin et al., 1987).

Z-RNA displays a well-organized network of tightly bound water molecules spanning the minor groove, with a Na^+ ion proposed to occupy the helical central position of the RNA backbone (Figures 3A, 3B, and 4B). On the other hand, the hydration structure in Z-DNA appears more variable (Gessner et al., 1989), and only the W1 water position is clearly shared between the two conformations. Moreover, in the Zα/Z-DNA complex, a water molecule is found to be bound by the cytosine base O2 atoms at a position equivalent (albeit more distant by 0.4–0.6 Å) to that of the Na^+ ions. A structure cannot provide a quantitative measure of the stability of the given conformation; however, it can be said qualitatively that Z-RNA displays several additional interactions that are likely to increase its stability relative to Z-DNA. It is well known that ribose rings usually maintain a C3′-endo sugar pucker, largely due to the presence of the 2′ hydroxyl group. Under some conditions of local stress—in selected positions of the $tRNA^{Phe}$ chain, for example—the C2′-endo pucker is adopted and is often due to intercalation (Rich et al., 1980). Systematic use of C2′-endo pucker is somewhat destabilizing, and the cytidine residues in the Z-RNA structure are found with that pucker. Thus, it appears that every other residue in Z-RNA is destabilizing, while, at the same time, the systematic solvation of the cytosine 2′-OH group (Figure 3A) has a stabilizing influence. The net energy balance between stability associated with significantly increased solvation and instability of the C2′-endo sugars is likely to determine the behavior of Z-RNA. It is possible that the difficulty in inducing the Z-RNA conformation reflects a higher energy barrier and a more stable starting conformation for A-RNA (Lesnik and Freier, 1995) rather than an unstable Z-RNA, as has often been assumed. The RNA A-to-Z transition is strongly temperature dependent (Hall et al., 1984), as opposed to the relative temperature independence of the equivalent DNA B-to-Z transition. It is likely that increasing temperature effectively surmounts the energy barrier separating two otherwise rather stable conformations.

EXPERIMENTAL PROCEDURES

A $(His)_6$-tagged Zα construct of hADAR1, comprising residues G136–Q202, was expressed in BL21 (DE3) *Escherichia coli* by using the Overnight Express AutoInduction System from Novagen. Cells from a 4 liter culture were chemically lysed, and the supernatant was applied to a Ni-NTA column. The column was washed with 5 mM imidazole and eluted with 300 mM imidazole. The eluted protein was dialyzed against thrombin buffer (5 mM Tris-HCl [pH 8.0], 37.5 mM NaCl, 62.5 mM $CaCl_2$, and 0.5 mM 2-mercaptoethanol) for 6 hr, and 20 U thrombin was added to the dialysis bag in order to cleave the N-terminal His tag. After 16 hr in thrombin, the protein was reloaded on the Ni-NTA column in order to remove any uncleaved molecules. The flowthrough was concentrated and applied to a Mono-S FPLC column. Zα was eluted with a 50–500 mM NaCl gradient and was subsequently dialyzed and concentrated to 1.45 mM in storage buffer (10 mM HEPES [pH 7.4], 20 mM NaCl).

The synthetic RNA $dUr(CG)_3$ obtained from Dharmacon (Boulder, CO, USA) was deprotected with 2′-deprotection buffer (100 mM acetic acid adjusted to pH 3.8 with TEMED) and lyophilized. The oligonucleotide was resuspended in storage buffer (10 mM HEPES [pH 7.4], 20 mM NaCl) to a final concentration of 3.6 mM (single strand) and was incubated at 80°C for 10 min, followed by slow cooling to room temperature overnight.

The Zα-$(dUr[CG]_3)$ complex was formed by mixing 0.6 mM protein with 0.3 mM dsRNA. This mixture was incubated at 37°C for 1 hr prior to setting up the crystallization trials. Crystals of the complex were obtained by the hanging-drop method, with each drop containing 2 μl of the Zα-$dUr(CG)_3$ mixture and 1 μl reservoir solution. The drops were equilibrated at room temperature against a reservoir containing 100 mM sodium acetate (pH 3.6) and 40% PEG 600. The best-diffracting crystals were obtained by microseeding in a 4 μl complex plus 2 μl reservoir drop equilibrated against 100 mM sodium acetate (pH 3.6) and 35% PEG 600. Needle-like crystals with dimensions of 0.05 mm × 0.05 mm × 0.4 mm appeared after 2 days and continued to grow for about 3 weeks.

Crystals of the Zα/RNA complex were directly frozen in liquid nitrogen. Data were collected at beamline 19-ID of the Advanced Photon Source (APS) of Argonne National Laboratory with an ADSC Quantum 315 detector. Data processing was done with MOSFLM (Leslie, 1999),

part of the CCP4 package (CCP4, 1994), and data were scaled with SCALA (Kabsch, 1988). Molecular replacement was performed by using the complex Zα/Z-DNA as a search model (PDB code 1QBJ) with EPMR (Kissinger et al., 1999). The resulting model from molecular replacement was used for rigid-body refinement with REFMAC (Murshudov et al., 1997) and was then modified to RNA and fitted into density with XTALVIEW (McRee, 1999). Repeated cycles of maximum-likelihood refinement and model fitting of omit maps by using REFMAC and XTALVIEW resulted in a model and density that allowed fitting of the 5′ overhanging base as well as a few amino- and carboxy-terminal residues not visible in the initial maps. Toward the end of the refinement we observed that one water molecule consistently refined to a distinctly low B factor value of 4 $Å^2$. We replaced this water molecule with different metal ions and subjected the model to refinement. Sodium ions converged to a B factor of 14.3 $Å^2$, K^+ converged to 28.1 $Å^2$, Ni^{2+} converged to 43.9 $Å^2$, and Zn^{2+} converged to 46.9 $Å^2$. Taking into account the average B factor of 12.6 $Å^2$ for the atoms that the metal ion is bound to, the shortest distance from an interacting atom (2.5 Å), and the fact that sodium is formally the only metal ion present in the crystallization mother liquor, we concluded that this position is occupied by a Na^+ ion. The two sodium ions present at the RNA backbone display an octahedral configuration, and distances from the non-solvent-coordinating atoms range from 2.3 to 2.6 Å. The final model has an R factor of 19.4% (R_{free} of 24.7%) and includes 160 solvent molecules. The N terminus is missing 1 and 3 residues from monomers A and B, respectively, while the C terminus is missing 4 and 1. Analysis of the RNA conformation was performed with 3DNA (Lu and Olson, 2003). The sequences that appear in Figure 2 were derived from the protein sequence entries with accession codes: P55265 (ADAR1), NP_073419 (E3L), and Q9QY24 (DLM-1) and the nucleotide sequence entry with accession code AU301066 (PKZ). Sequence alignments were performed with ClustalW (Higgins and Sharp, 1988). Visualization, the production of figures, and model study were done with PYMOL (DeLano, 2002). For the structural comparisons, we performed we used the PDB entries 1T4X (model 1) for the high-salt NMR structure and 1QBJ for the Zα/Z-DNA complex.

Supplemental Data

Supplemental Data include comparison of pseudo rotation angles of Z-RNA, Z-DNA (bound by Zα), and Z-RNA in high salt (Table S1) and detailed parameters defining sugar conformation in the Zα/RNA complex (Table S2) and are available at http://www.structure.org/cgi/content/full/15/4/395/DC1/.

ACKNOWLEDGMENTS

We thank Dr. Jerzy Osipiuk at the Argon Photon Source for his help in data collection. We also thank Prof. Cathy Drennan and people of her lab for valuable discussion and help during data collection. During part of this project, A.A. was supported by the Human Frontiers Science Program, and B.A.B., II was supported by an Aid for Cancer Research Postoctoral Fellowship. D.P. is a recipient of a grant from FCT (Fundacao para a Ciencia e Tecnologia [SFRH/BD/14384/2003]). During part of this work, D.P. was partially supported by FLAD (Luso-American Foundation). This research was supported by grants from the National Institutes of Health and the Ellison Foundation. A.R., A.A., and D.P. conceived and designed the experiments; K.L. purified Zα on FPLC; B.B. performed initial crystallization experiments; D.P. obtained and optimized the crystals; D.P. and A.A. collected and analyzed the data; A.A. and D.P. determined the structure; and A.A., A.R., and D.P. wrote the paper.

Received: November 21, 2006
Revised: February 27, 2007
Accepted: March 2, 2007
Published: April 17, 2007

REFERENCES

Athanasiadis, A., Placido, D., Maas, S., Brown, B.A., 2nd, Lowenhaupt, K., and Rich, A. (2005). The crystal structure of the Zβ domain of the RNA-editing enzyme ADAR1 reveals distinct conserved surfaces among Z-domains. J. Mol. Biol. *351*, 496–507.

Brown, B.A., 2nd, Lowenhaupt, K., Wilbert, C.M., Hanlon, E.B., and Rich, A. (2000). The zα domain of the editing enzyme dsRNA adenosine deaminase binds left-handed Z-RNA as well as Z-DNA. Proc. Natl. Acad. Sci. USA *97*, 13532–13536.

Cattaneo, R. (1994). Biased (A→I) hypermutation of animal RNA virus genomes. Curr. Opin. Genet. Dev. *4*, 895–900.

CCP4 (Collaborative Computational Project, Number 4) (1994). The CCP4 suite: programs for protein crystallography. Acta Crystallogr. D Biol. Crystallogr. *50*, 760–763.

Davis, P.W., Adamiak, R.W., and Tinoco, I., Jr. (1990). Z-RNA: the solution NMR structure of r(CGCGCG). Biopolymers *29*, 109–122.

DeLano, W.L. (2002). The PyMOL Molecular Graphics System (http://www.pymol.org).

George, C.X., and Samuel, C.E. (1999). Human RNA-specific adenosine deaminase ADAR1 transcripts possess alternative exon 1 structures that initiate from different promoters, one constitutively active and the other interferon inducible. Proc. Natl. Acad. Sci. USA *96*, 4621–4626.

Gessner, R.V., Frederick, C.A., Quigley, G.J., Rich, A., and Wang, A.H. (1989). The molecular structure of the left-handed Z-DNA double helix at 1.0 Å atomic resolution. Geometry, conformation, and ionic interactions of d(CGCGCG). J. Biol. Chem. *264*, 7921–7935.

Hall, K., Cruz, P., Tinoco, I., Jr., Jovin, T.M., and van de Sande, J.H. (1984). 'Z-RNA'—a left-handed RNA double helix. Nature *311*, 584–586.

Hardin, C.C., Zarling, D.A., Puglisi, J.D., Trulson, M.O., Davis, P.W., and Tinoco, I., Jr. (1987). Stabilization of Z-RNA by chemical bromination and its recognition by anti-Z-DNA antibodies. Biochemistry *26*, 5191–5199.

Herbert, A., Alfken, J., Kim, Y.G., Mian, I.S., Nishikura, K., and Rich, A. (1997). A Z-DNA binding domain present in the human editing enzyme, double-stranded RNA adenosine deaminase. Proc. Natl. Acad. Sci. USA *94*, 8421–8426.

Higgins, D.G., and Sharp, P.M. (1988). CLUSTAL: a package for performing multiple sequence alignment on a microcomputer. Gene *73*, 237–244.

Horikami, S.M., and Moyer, S.A. (1995). Double-stranded RNA adenosine deaminase activity during measles virus infection. Virus Res. *36*, 87–96.

Kabsch, W. (1988). Evaluation of single-crystal X-ray diffraction data from a position-sensitive detector. J. Appl. Cryst. *21*, 916–924.

Kahmann, J.D., Wecking, D.A., Putter, V., Lowenhaupt, K., Kim, Y.G., Schmieder, P., Oschkinat, H., Rich, A., and Schade, M. (2004). The solution structure of the N-terminal domain of E3L shows a tyrosine conformation that may explain its reduced affinity to Z-DNA in vitro. Proc. Natl. Acad. Sci. USA *101*, 2712–2717.

Kim, Y.G., Lowenhaupt, K., Oh, D.B., Kim, K.K., and Rich, A. (2004). Evidence that vaccinia virulence factor E3L binds to Z-DNA in vivo: implications for development of a therapy for poxvirus infection. Proc. Natl. Acad. Sci. USA *101*, 1514–1518.

Kissinger, C.R., Gehlhaar, D.K., and Fogel, D.B. (1999). Rapid automated molecular replacement by evolutionary search. Acta Crystallogr. D Biol. Crystallogr. *55*, 484–491.

Koeris, M., Funke, L., Shrestha, J., Rich, A., and Maas, S. (2005). Modulation of ADAR1 editing activity by Z-RNA in vitro. Nucleic Acids Res. *33*, 5362–5370.

Leslie, A.G. (1999). Integration of macromolecular diffraction data. Acta Crystallogr. D Biol. Crystallogr. *55*, 1696–1702.

Lesnik, E.A., and Freier, S.M. (1995). Relative thermodynamic stability of DNA, RNA, and DNA:RNA hybrid duplexes: relationship with base composition and structure. Biochemistry *34*, 10807–10815.

Liu, L.F., and Wang, J.C. (1987). Supercoiling of the DNA template during transcription. Proc. Natl. Acad. Sci. USA *84*, 7024–7027.

Liu, Y., Lei, M., and Samuel, C.E. (2000). Chimeric double-stranded RNA-specific adenosine deaminase ADAR1 proteins reveal functional selectivity of double-stranded RNA-binding domains from ADAR1 and protein kinase PKR. Proc. Natl. Acad. Sci. USA *97*, 12541–12546.

Lu, X.J., and Olson, W.K. (2003). 3DNA: a software package for the analysis, rebuilding and visualization of three-dimensional nucleic acid structures. Nucleic Acids Res. *31*, 5108–5121.

McRee, D.E. (1999). XtalView/Xfit—a versatile program for manipulating atomic coordinates and electron density. J. Struct. Biol. *125*, 156–165.

Murshudov, G.N., Vagin, A.A., and Dodson, E.J. (1997). Refinement of macromolecular structures by the maximum-likelihood method. Acta Crystallogr. D Biol. Crystallogr. *53*, 240–255.

Nakamura, Y., Fujii, S., Urata, H., Uesugi, S., Ikehara, M., and Tomita, K. (1985). Crystal structure of a left-handed RNA tetramer, r(C-br8G)2. Nucleic Acids Symp. Ser. *16*, 29–32.

Pohl, F.M., and Jovin, T.M. (1972). Salt-induced co-operative conformational change of a synthetic DNA: equilibrium and kinetic studies with poly (dG-dC). J. Mol. Biol. *67*, 375–396.

Polson, A.G., Bass, B.L., and Casey, J.L. (1996). RNA editing of hepatitis delta virus antigenome by dsRNA-adenosine deaminase. Nature *380*, 454–456.

Popenda, M., Milecki, J., and Adamiak, R.W. (2004). High salt solution structure of a left-handed RNA double helix. Nucleic Acids Res. *32*, 4044–4054.

Rich, A., Wang, A.J., and Quigley, G.J. (1980). Diversity of sugar pucker in the nucleic acids. In Frontiers of Bioorganc Chemistry and Molecular Biology, S.N. Ananchenko, ed. (Oxford: Pergamon Press), pp. 327–337.

Robertson, H.D., and Mathews, M.B. (1996). The regulation of the protein kinase PKR by RNA. Biochimie *78*, 909–914.

Rothenburg, S., Deigendesch, N., Dittmar, K., Koch-Nolte, F., Haag, F., Lowenhaupt, K., and Rich, A. (2005). A PKR-like eukaryotic initiation factor 2α kinase from zebrafish contains Z-DNA binding domains instead of dsRNA binding domains. Proc. Natl. Acad. Sci. USA *102*, 1602–1607.

Scadden, A.D. (2005). The RISC subunit Tudor-SN binds to hyper-edited double-stranded RNA and promotes its cleavage. Nat. Struct. Mol. Biol. *12*, 489–496.

Schade, M., Turner, C.J., Kuhne, R., Schmieder, P., Lowenhaupt, K., Herbert, A., Rich, A., and Oschkinat, H. (1999). The solution structure of the Zα domain of the human RNA editing enzyme ADAR1 reveals a prepositioned binding surface for Z-DNA. Proc. Natl. Acad. Sci. USA *96*, 12465–12470.

Schwartz, T., Rould, M.A., Lowenhaupt, K., Herbert, A., and Rich, A. (1999). Crystal structure of the Zα domain of the human editing enzyme ADAR1 bound to left-handed Z-DNA. Science *284*, 1841–1845.

Schwartz, T., Behlke, J., Lowenhaupt, K., Heinemann, U., and Rich, A. (2001). Structure of the DLM-1-Z-DNA complex reveals a conserved family of Z-DNA-binding proteins. Nat. Struct. Biol. *8*, 761–765.

Stefl, R., Xu, M., Skrisovska, L., Emeson, B.R., and Allain, H.-T.F. (2006). Structure and specific RNA binding of ADAR2 double-stranded RNA binding motifs. Structure *14*, 345–355.

Taylor, D.R., Puig, M., Darnell, M.E., Mihalik, K., and Feinstone, S.M. (2005). New antiviral pathway that mediates hepatitis C virus replicon interferon sensitivity through ADAR1. J. Virol. *79*, 6291–6298.

Teng, M.K., Liaw, Y.C., van der Marel, G.A., van Boom, J.H., and Wang, A.H. (1989). Effects of the O2′ hydroxyl group on Z-DNA conformation: structure of Z-RNA and (araC)-[Z-DNA]. Biochemistry *28*, 4923–4928.

Tonkin, L.A., and Bass, B.L. (2003). Mutations in RNAi rescue aberrant chemotaxis of ADAR mutants. Science *302*, 1725.

Trulson, M.O., Cruz, P., Puglisi, J.D., Tinoco, I., Jr., and Mathies, R.A. (1987). Raman spectroscopic study of left-handed Z-RNA. Biochemistry *26*, 8624–8630.

Wang, A.H., Quigley, G.J., Kolpak, F.J., Crawford, J.L., van Boom, J.H., van der Marel, G., and Rich, A. (1979). Molecular structure of a left-handed double helical DNA fragment at atomic resolution. Nature *282*, 680–686.

Wang, A.J., Quigley, G.J., Kolpak, F.J., van der Marel, G., van Boom, J.H., and Rich, A. (1981). Left-handed double helical DNA: variations in the backbone conformation. Science *211*, 171–176.

Wittig, B., Dorbic, T., and Rich, A. (1991). Transcription is associated with Z-DNA formation in metabolically active permeabilized mammalian cell nuclei. Proc. Natl. Acad. Sci. USA *88*, 2259–2263.

Yang, W., Wang, Q., Howell, K.L., Lee, J.T., Cho, D.S., Murray, J.M., and Nishikura, K. (2005). ADAR1 RNA deaminase limits short interfering RNA efficacy in mammalian cells. J. Biol. Chem. *280*, 3946–3953.

Zarling, D.A., Calhoun, C.J., Feuerstein, B.G., and Sena, E.P. (1990). Cytoplasmic microinjection of immunoglobulin Gs recognizing RNA helices inhibits human cell growth. J. Mol. Biol. *211*, 147–160.

Accession Numbers

The coordinates and structure factors have been deposited in the Research Collaboratory for Structural Bioinformatics database and have been assigned PDB ID 2GXB, NDB ID PR0210, and RCSB ID RCSB037662.

